ORBITER ENTRY TRAJECTORY CONSIDERATIONS

By John J. Rehder and Paul F. Holloway

NASA Langley Research Center

INTRODUCTION

Any space shuttle trajectory-shaping optimization study must consider the vehicle's thermal environment and the resulting requirements of the thermal protection system (TPS). Optimization studies have been conducted at the NASA Langley Research Center, yielding results which are generally applicable to shuttle orbiters and are independent of evolution and redirection of the space shuttle program. This paper presents the work of two investigations of optimal trajectory shaping, in which different methods of considering the thermal environment are used.

The first approach defines a nominal trajectory which achieves a desired cross range by assuming a simple control history with an appropriate TPS design. Trajectory optimization is then used to maximize cross range with minimal impact on the nominal TPS. Heating analysis illustrates the effect of the optimization on surface temperatures and heat-load distribution along the bottom center line of the vehicle. This approach indicates the mission flexibility and growth potential in terms of cross-range capability which may be realized through trajectory shaping.

The goal of the second study is to determine if payload gains for an all-ablative TPS Mark I orbiter can result from entry trajectory optimization. Since the ablative TPS weight is primarily a function of heat load, the total stagnation-point heat load is minimized for various values of cross range and deorbit propellant weight. The effects on total weight (ablator + propellant) are summarized.

The aerodynamic characteristics in both studies are typical of delta-wing orbiter configurations. Entry is initiated from an equatorial orbit at an altitude of 185.2 km at 0° latitude and longitude. Entry into the atmosphere occurs at 121.9 km.

SYMBOLS

C_L	lift coefficient
$f(\alpha)$	experimentally determined boundary layer transition onset prediction as a function of angle of attack
I_{sp}	specific impulse
L	length of vehicle
M	Mach number
Q_{total}	total heat load

Re_θ	Reynolds number based on momentum thickness
S	reference area
T	temperature
V	velocity
W	weight of vehicle
x	distance along center line of vehicle with the nose as origin
α	angle of attack, deg
μ	coefficient of viscosity
ρ	density
ϕ	bank angle, deg

Subscripts:

e	edge of boundary layer
max	maximum

MAXIMIZING CROSS RANGE WITH MINIMAL IMPACT ON AERODYNAMIC HEATING AND TPS

During space shuttle operations, it may be desirable to obtain a cross range greater than the design nominal with minimal impact on TPS weight or material. The approach followed defines a nominal entry trajectory for the initial operational period of the orbiter. A simple control history – constant angle of attack and simple bank-angle variation – and an appropriate TPS are assumed. The optimal angle-of-attack and bank-angle histories are then determined which will maximize cross range with the maximum heat rate and total heat load at the stagnation point constrained to those of the nominal.

In all trajectories the maximum deceleration was limited to 3g (1g = 9.8 m/sec^2). The vehicle characteristics, which are typical of fully reusable orbiter designs, include a weight of 102 060 kg and a reference area of 565.2 m^2. An entry angle of -1.6° and entry velocity of 7450 m/sec were assumed.

HEATING ASSUMPTIONS

A heating analysis along the bottom center line of the vehicle for all trajectories was conducted using the MINIVER computer program developed by the McDonnell Douglas Astronautics Company (MDAC). Laminar and turbulent heat-transfer calculations for a flat plate were based on the Eckert reference enthalpy method and Spalding and Chi method, respectively. Sharp-cone conditions (oblique shock entropy) were used to determine shock angle and local flow conditions.

The onset of boundary-layer transition was predicted using both the current MDAC and North American Rockwell Corporation (NAR) criteria. For the MDAC criteria, transition onset occurs when $\frac{Re_\theta}{M_e}\left(\frac{\rho_e V_e}{\mu_e}\right)^{-0.2}$ lies on the experimentally determined curve $f(\alpha)$. The NAR criteria predicts transition onset when $\frac{Re_\theta}{M_e} = 225$. For both cases, fully turbulent flow was assumed to occur at a length Reynolds number double that at transition onset. The Baranowski crossflow correction accounts for the effects of streamline divergence on a delta-wing configuration in a real gas. The calculation of thin-skin surface temperatures was based on the material characteristics of coated columbium.

ENTRY TRAJECTORY CONTROL HISTORIES – LOW CROSS RANGE

The nominal trajectory was flown at a constant angle of attack of 53° at $C_{L,max}$. The vehicle banks at pull-out, and the bank angle decreases at a constant rate. The nominal trajectory obtains a cross range of 240 n.mi. (See fig. 1.)

The optimal trajectory begins the bank program earlier and maintains a steeper bank throughout most of the entry. Once the vehicle has decelerated sufficiently, the angle of attack is modulated downward to increase range without violating the heating-rate constraint. The steeper bank angles also result in a more efficient heading-angle change which is the primary factor in increasing the cross range to 571 n.mi.

The quantitative increase in cross range is not important, since this percentage is governed by the selection of the nominal entry profile. The results do establish qualitatively, however, that significant increases in ranging are possible through optimal trajectory shaping.

ENTRY TRAJECTORY CONTROL HISTORIES

LOW CROSS RANGE

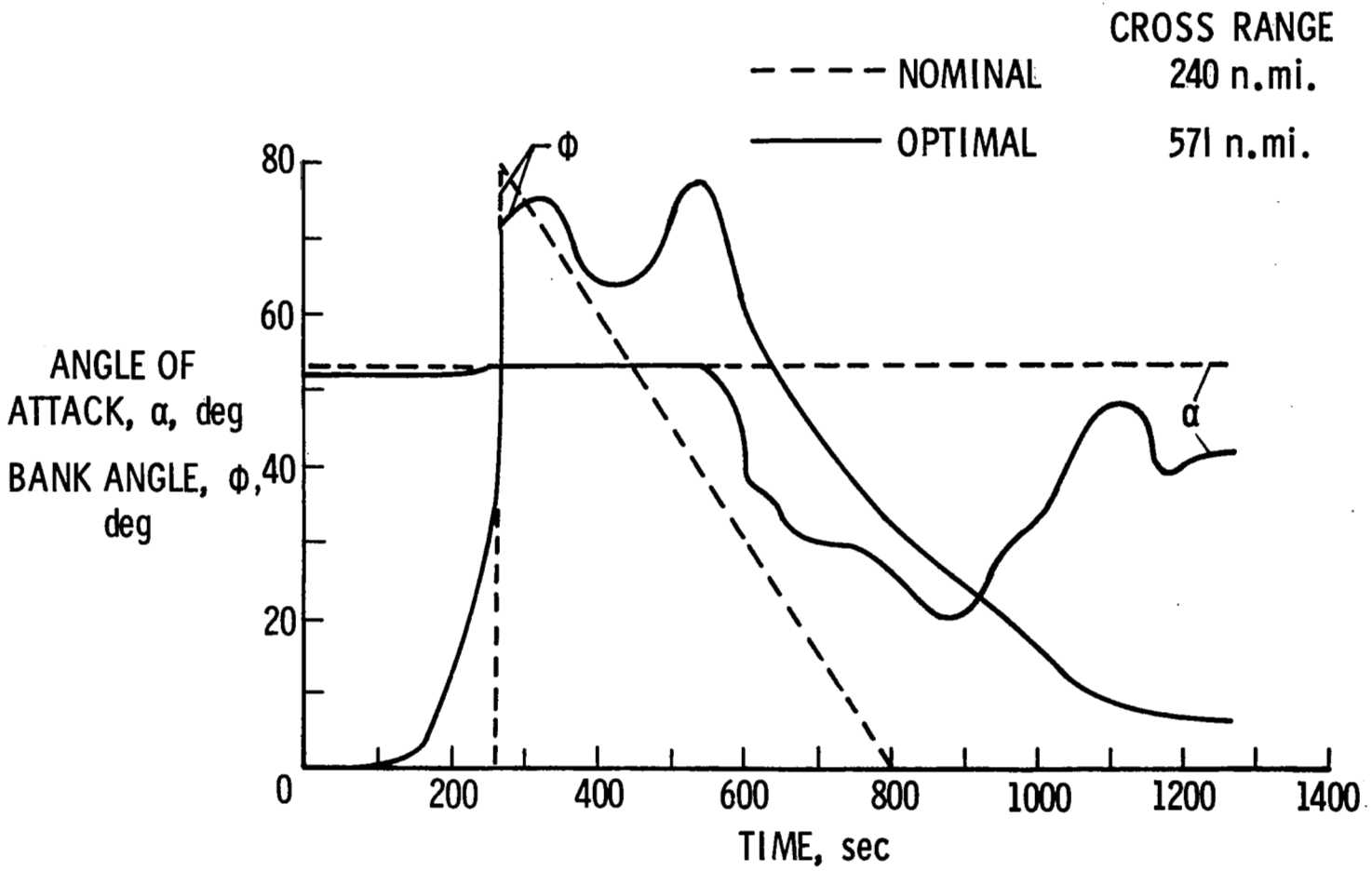

Figure 1

ALTITUDE AND VELOCITY HISTORIES – LOW CROSS RANGE

A comparison of the nominal and optimal altitude and velocity time histories is given in figure 2. The earlier and steeper bank-angle history of the optimal trajectory results in quicker deceleration yielding a lower altitude profile at slower speeds at any time over most of the entry.

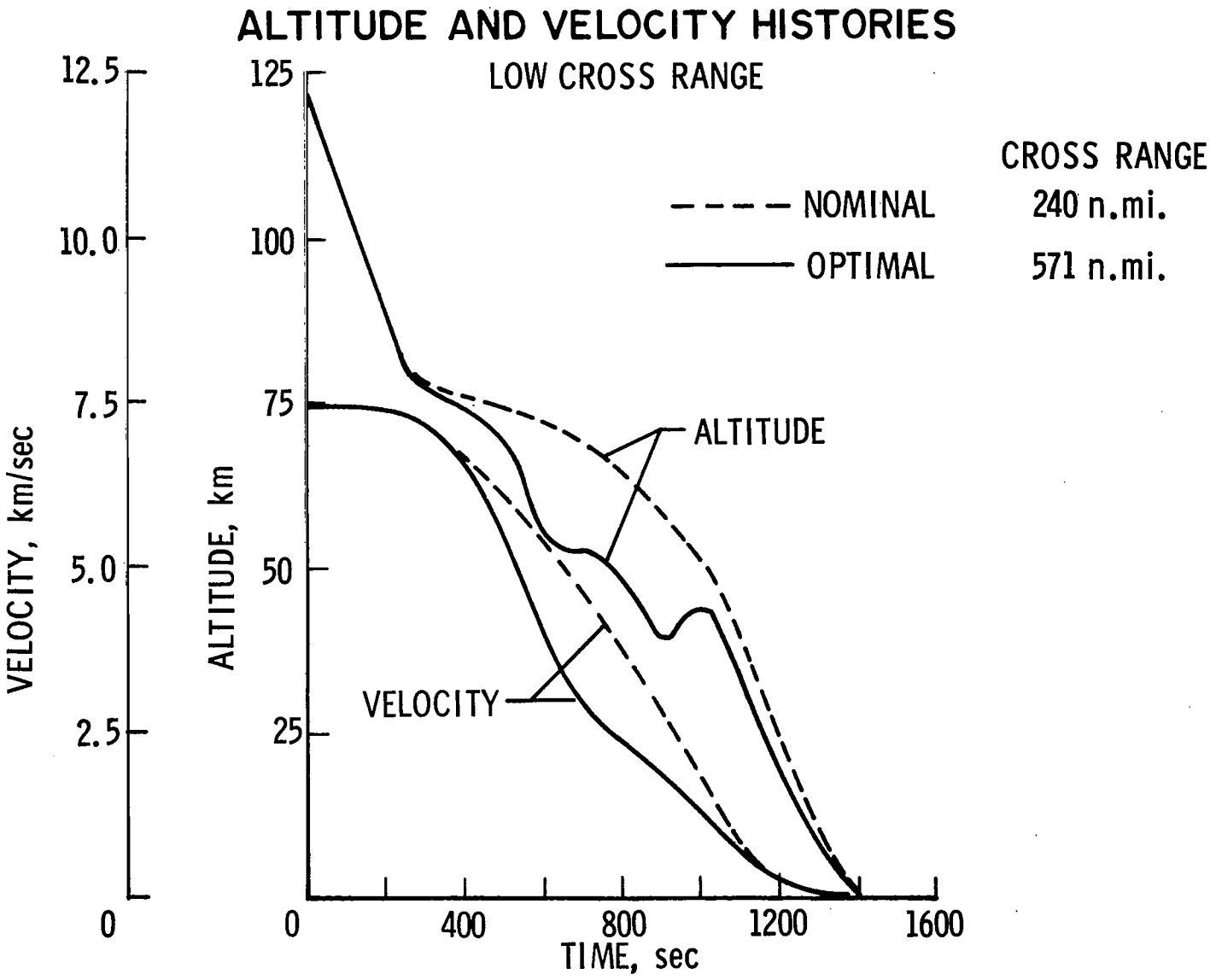
ALTITUDE AND VELOCITY HISTORIES
LOW CROSS RANGE
CROSS RANGE
NOMINAL 240 n.mi.
OPTIMAL 571 n.mi.
ALTITUDE
VELOCITY
VELOCITY, km/sec
ALTITUDE, km
TIME, sec
12.5
10.0
7.5
5.0
2.5
0
125
100
75
50
25
0
400
800
1200
1600

Figure 2

STAGNATION-POINT HEATING SUMMARY – LOW CROSS RANGE

The results of the stagnation-point heat constraints are shown in figure 3. The heat rate for the optimal case remains near the maximum value for a longer period of time. Later in the entry, however, the optimal heat rates are less than those of the nominal so that the integrated heat loads are virtually the same for both cases.

STAGNATION-POINT HEATING SUMMARY
LOW CROSS RANGE

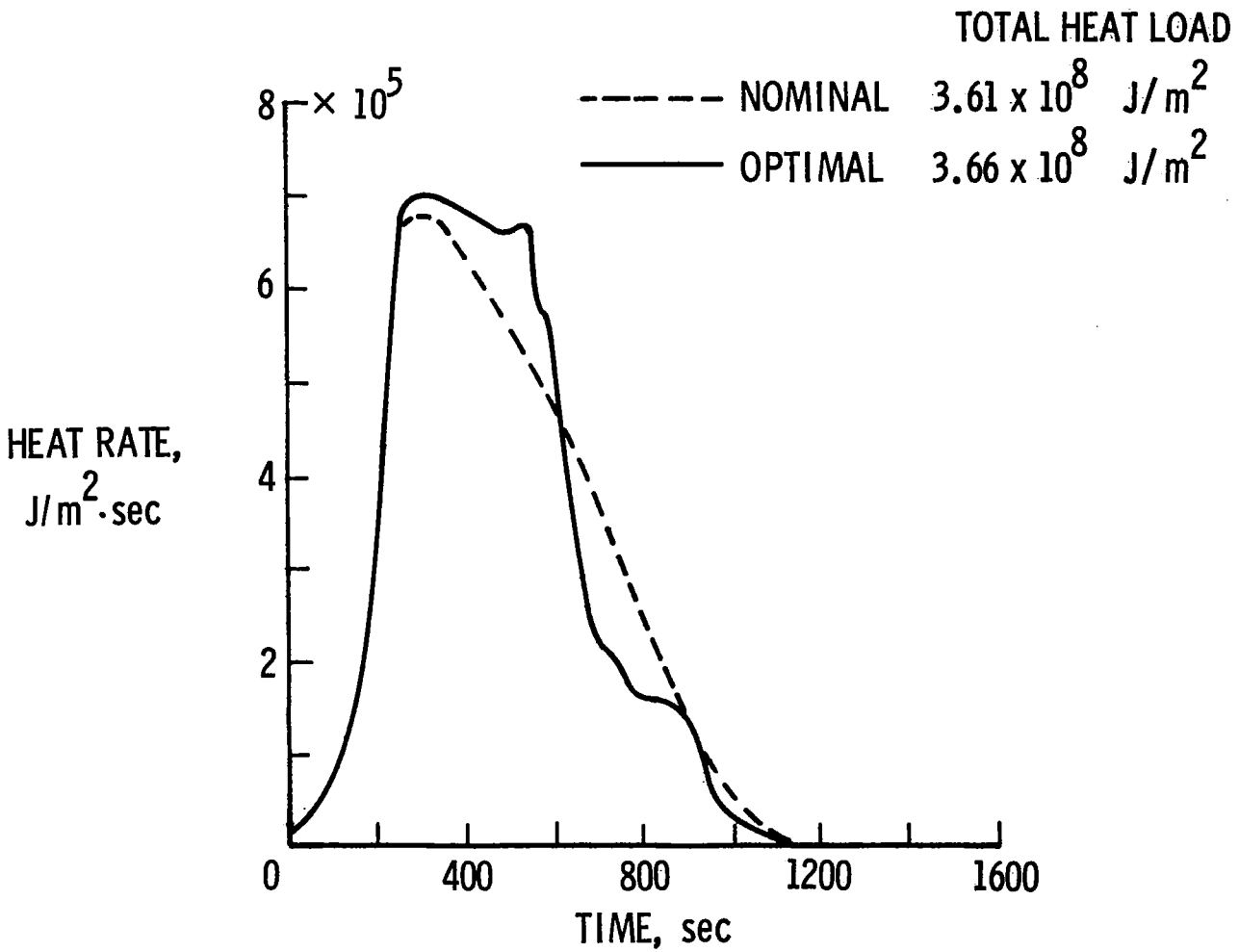

Figure 3

MAXIMUM BOTTOM CENTER-LINE TEMPERATURES – LOW CROSS RANGE

A comparison of the maximum surface-temperature distributions for the nominal and optimal trajectories is shown in figure 4 for both the MDAC and NAR boundary-layer transition criteria. The temperature limits for several candidate materials for reusable TPS designs are indicated on the right of the figure. The difference between the maximum temperatures for the MDAC transition criteria is 100° K or less over most of the vehicle with the optimal case having the higher temperatures. For the NAR criteria, there is no difference in maximum temperatures over the forward portion of the body, while the maximum temperatures encountered during the optimal trajectory on the rearward portion are about 400° K greater than those in the nominal trajectory. For the Haynes material, assuming MDAC criteria, and for the superalloys, assuming NAR criteria, optimal entry would not require a new surface material.

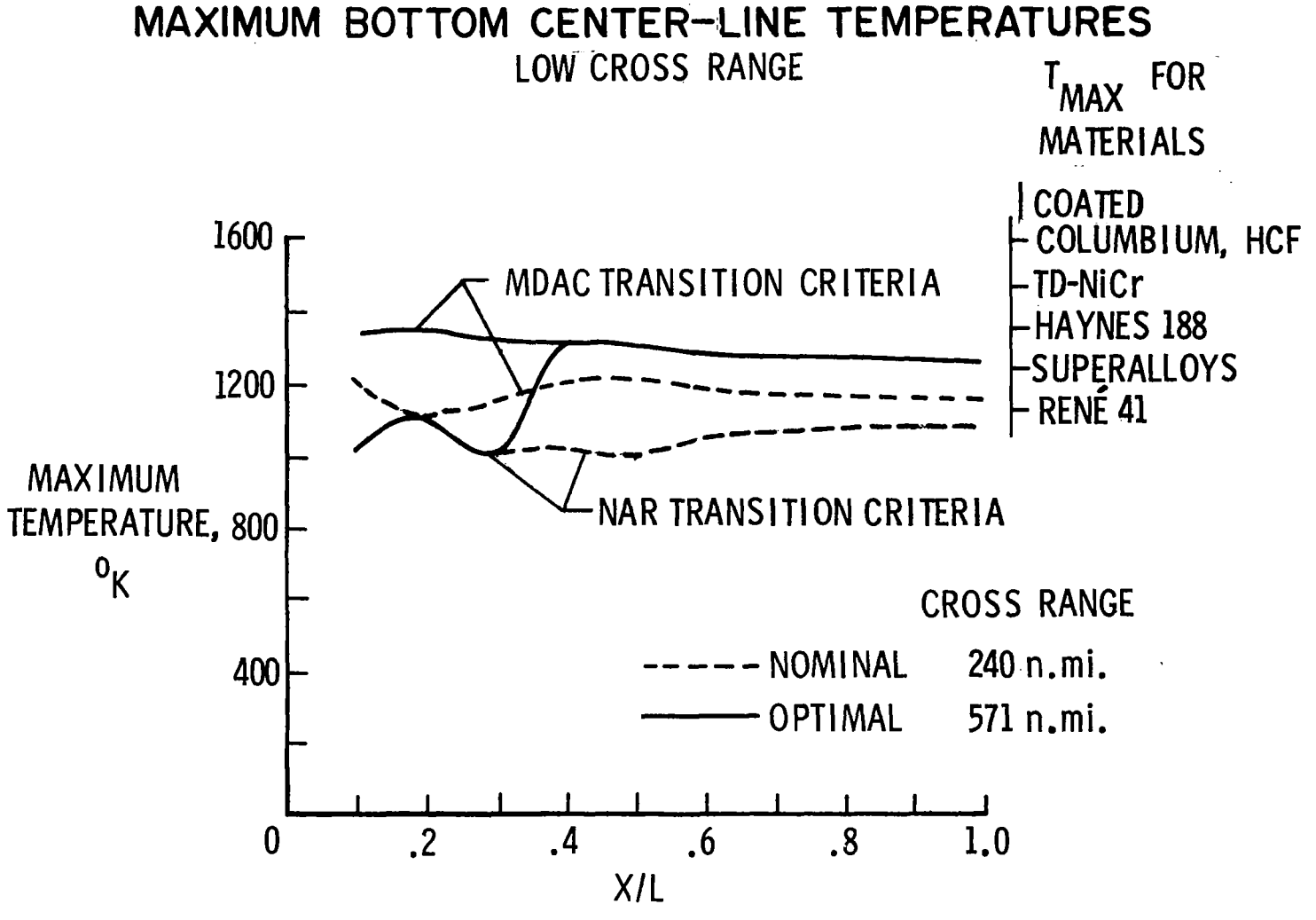
MAXIMUM BOTTOM CENTER-LINE TEMPERATURES
LOW CROSS RANGE
T_{MAX} FOR MATERIALS
COATED COLUMBIUM, HCF
TD-NiCr
HAYNES 188 SUPERALLOYS
RENÉ 41
MDAC TRANSITION CRITERIA
NAR TRANSITION CRITERIA
MAXIMUM TEMPERATURE, ^{o}K
1600
1200
800
400
0
.2
.4
.6
.8
1.0
X/L
CROSS RANGE
NOMINAL 240 n.mi.
OPTIMAL 571 n.mi.

Figure 4

BOTTOM CENTER-LINE CONVECTIVE HEAT SUMMARY – LOW CROSS RANGE

Significant differences in the total-heat-load distribution levels are indicated as a result of transition criteria. (See fig. 5.) Comparisons between the optimal and nominal trajectories indicate that the optimal heat load is slightly higher than the nominal over the forward portion of the vehicle using the MDAC transition criteria. Using the NAR criteria, the trend is reversed with the heat load for the nominal trajectory higher than that for the optimal trajectory on the forward portion of the body and lower on the rearward portion.

It should also be noted that the differences in heat load between the optimal and nominal entries predicted for either transition criteria are considerably less than the differences caused by the two criteria for a particular trajectory.

BOTTOM CENTER-LINE CONVECTIVE HEAT SUMMARY

LOW CROSS RANGE

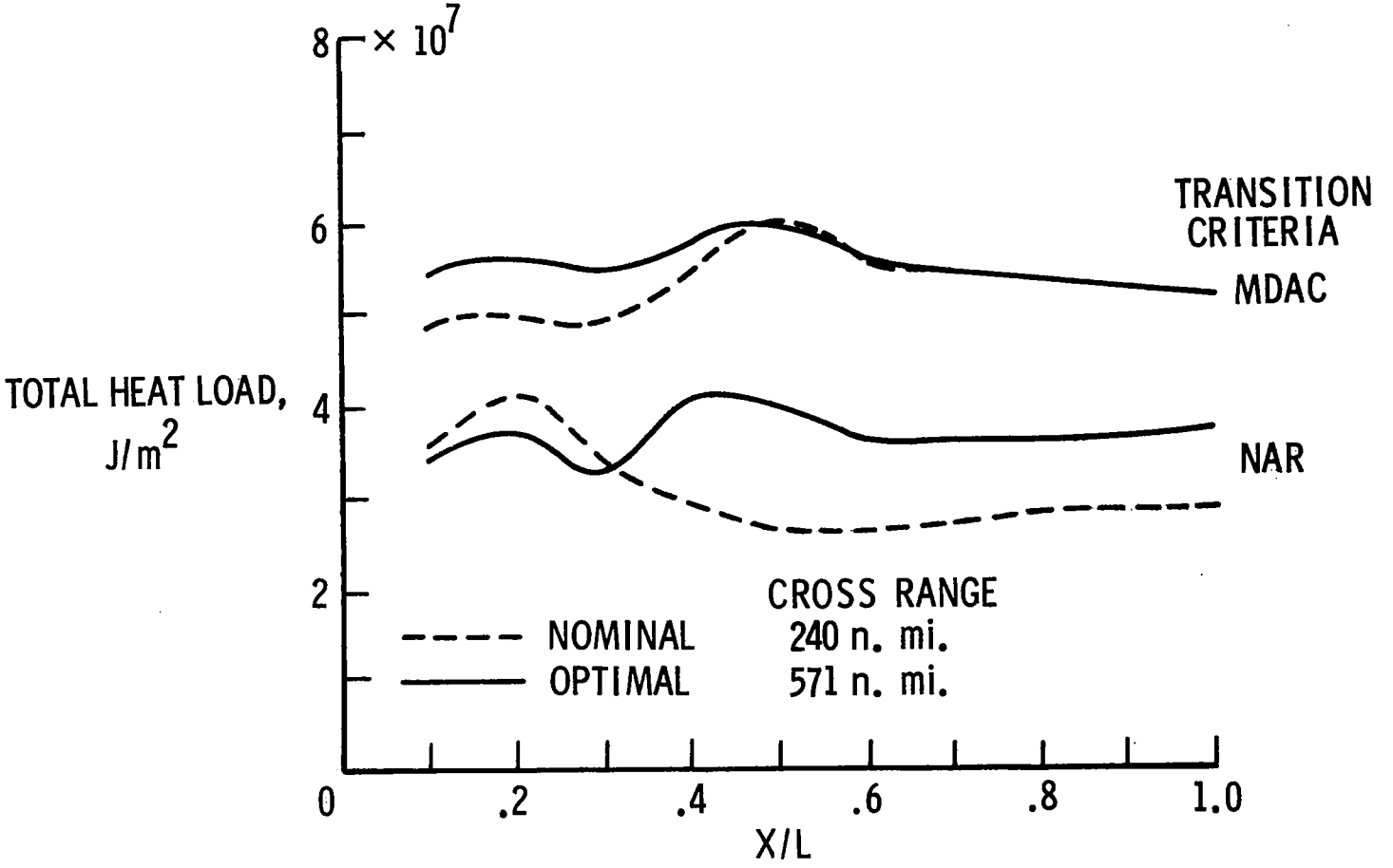

Figure 5

ENTRY TRAJECTORY COMPARISON – MEDIUM CROSS RANGE

A medium cross range nominal entry trajectory was generated using a constant angle of attack of 40° and another simple bank angle history. An optimal trajectory, maximizing cross range, was determined using the same technique previously described. The angle of attack, bank angle, altitude, velocity, and stagnation-point heat-rate histories, shown in figure 6, indicate the same characteristics as the low cross range case. Using the MDAC transition criteria, the maximum center-line temperature profiles were very similar to those shown previously, while the total heat load, in this case, is higher for the optimal trajectory across the entire bottom center line.

ENTRY TRAJECTORY COMPARISON—MEDIUM CROSS RANGE

	CROSS RANGE	TOTAL HEAT LOAD AT STAGNATION POINT
NOMINAL	587 n. mi.	------ 5.12×10^8 J/m^2
OPTIMAL	1014 n. mi.	——— 5.19×10^8 J/m^2

MDAC TRANSITION CRITERIA

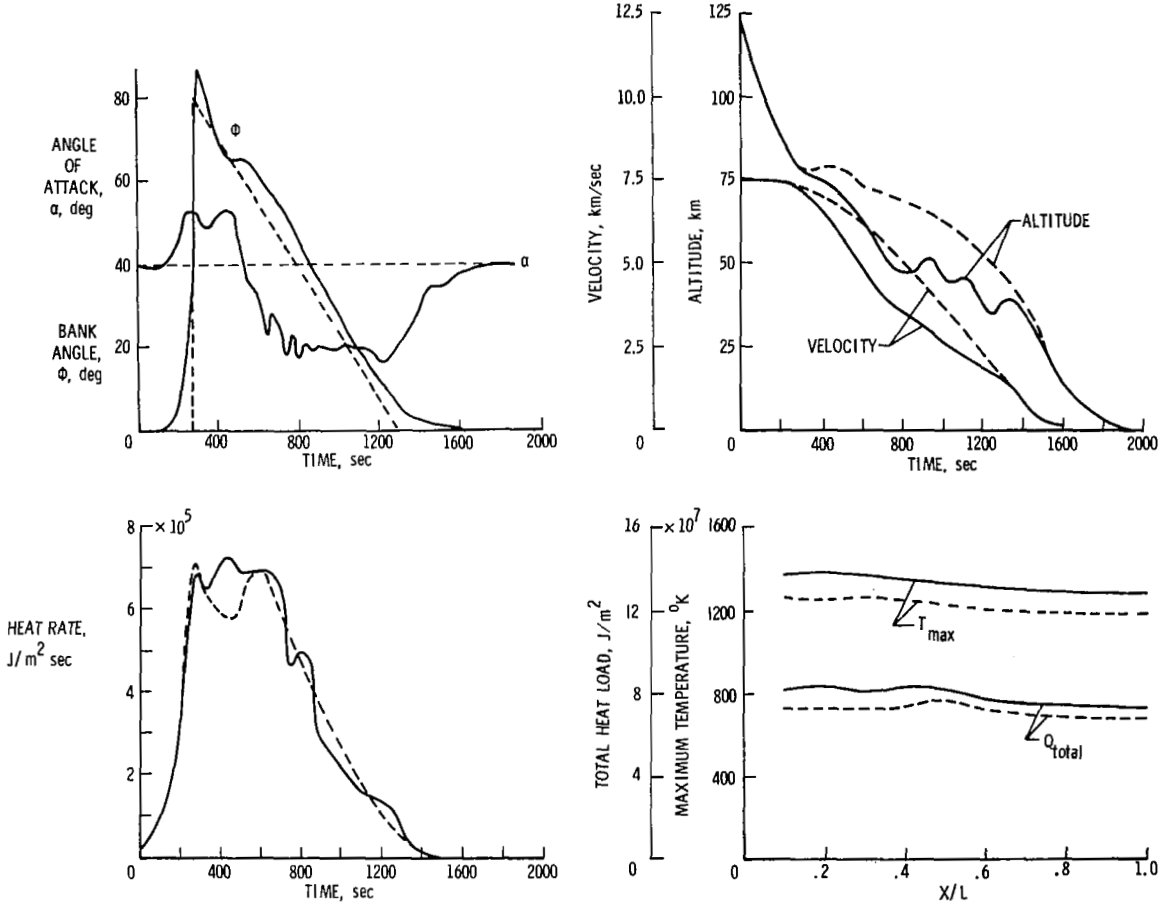

Figure 6

ENTRY TRAJECTORY COMPARISON – HIGH CROSS RANGE

The same process was followed using a nominal trajectory with a constant angle of attack of 30° and another simple bank-angle history. The improvement in cross range was not as great in this case. Otherwise the results, shown in figure 7, are entirely similar to those of the low cross range case.

ENTRY TRAJECTORY COMPARISON—HIGH CROSS RANGE

	CROSS RANGE	TOTAL HEAT LOAD AT STAGNATION POINT
NOMINAL	1107 n. mi.	------ 8.33×10^8 J/m^2
OPTIMAL	1470 n. mi.	——— 8.28×10^8 J/m^2

MDAC TRANSITION CRITERIA

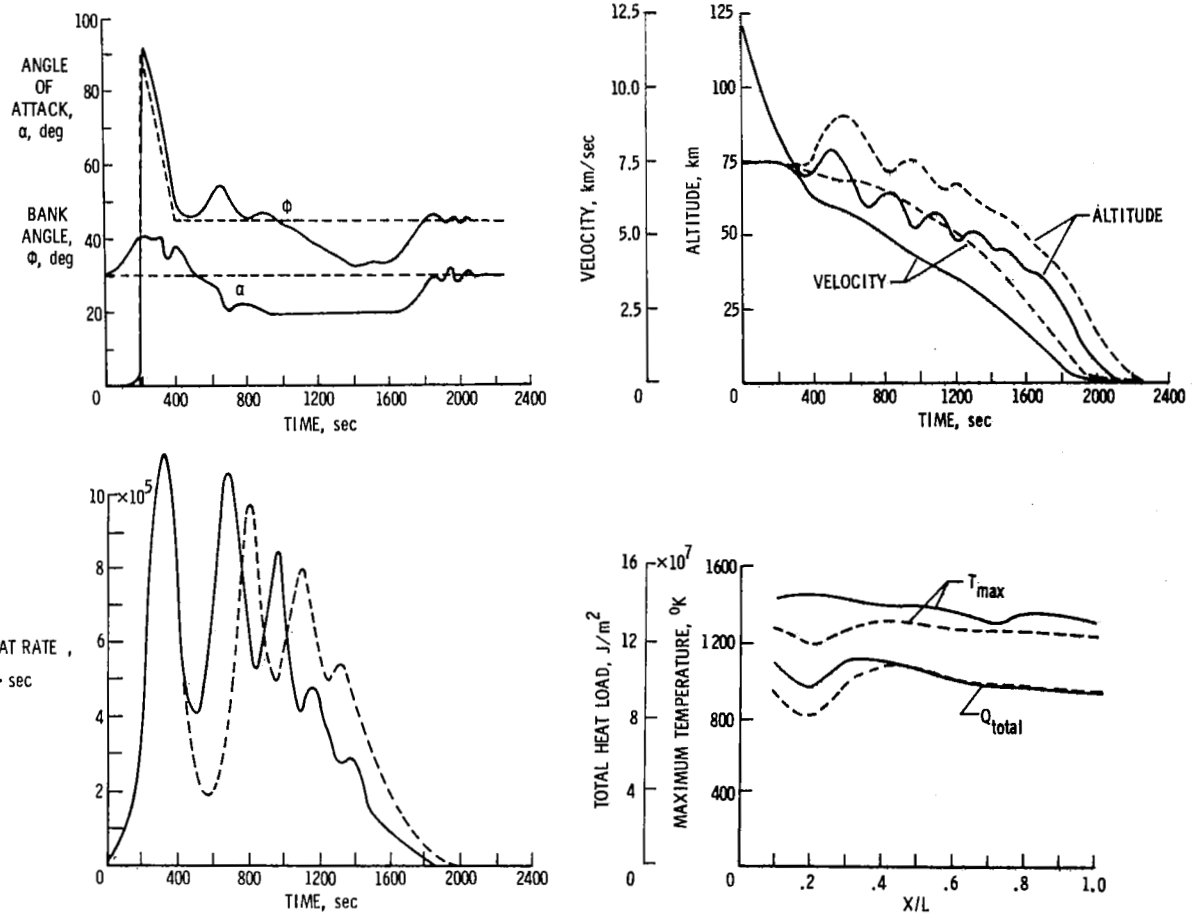

Figure 7

ENTRY TRAJECTORY OPTIMIZATION FOR SHUTTLE ORBITER WITH ABLATIVE TPS

The second objective of this study is to examine the possibility of gaining payload for a Mark I orbiter design through trajectory optimization for an all-ablative TPS. (See fig. 8.) In this analysis, minimum total stagnation-point heat-load trajectories are calculated for various values of cross range from 300 to 1500 n.mi. Since entry angle, or deorbit ΔV, plays a major role in determination of the total heat load, these effects are also investigated. In addition, an alternate entry mode using negative lift to steepen the flight path is evaluated.

Aerodynamic characteristics, weight, and reference area compatible with current Mark I orbiter designs are assumed. As in the preceding analysis, entry is initiated from an equatorial orbit at an altitude of 185.2 km at 0° latitude and longitude. Maximum deceleration was limited to 2.5g for all trajectories.

ENTRY TRAJECTORY OPTIMIZATION FOR SHUTTLE ORBITER WITH ABLATIVE TPS

PURPOSE

- DETERMINE MINIMUM TOTAL STAGNATION-POINT HEAT LOAD TRAJECTORIES AT VARIOUS CROSS RANGES AND ENTRY CONDITIONS FOR MARK I ORBITER
- STUDY EFFECT OF DEORBIT ΔV ON THE ENTRY WEIGHT OF THE VEHICLE
- INVESTIGATE ALTERNATE ENTRY MODES TO OBTAIN MINIMUM VEHICLE WEIGHT

ASSUMPTIONS

- MARK I ORBITER - ALL-ABLATIVE TPS
- WEIGHT = 68 267 kg
- REFERENCE AREA = 310.7 m^2

Figure 8

EFFECT OF ENTRY ANGLE ON STAGNATION-POINT HEATING

It is well known that for a given vehicle entering the atmosphere at a given angle of attack, the maximum stagnation-point heat rate increases as the entry angle increases, while the total heat load decreases because of lower flight time. (See fig. 9.)

Since an ablative TPS allows a relaxation of maximum heat-rate constraints, the possibility of reducing total heat load, thereby reducing TPS weight, by entering at a higher entry angle is investigated as a potential means of reducing vehicle weight and/or improving payload capability.

EFFECT OF ENTRY ANGLE ON STAGNATION-POINT HEATING

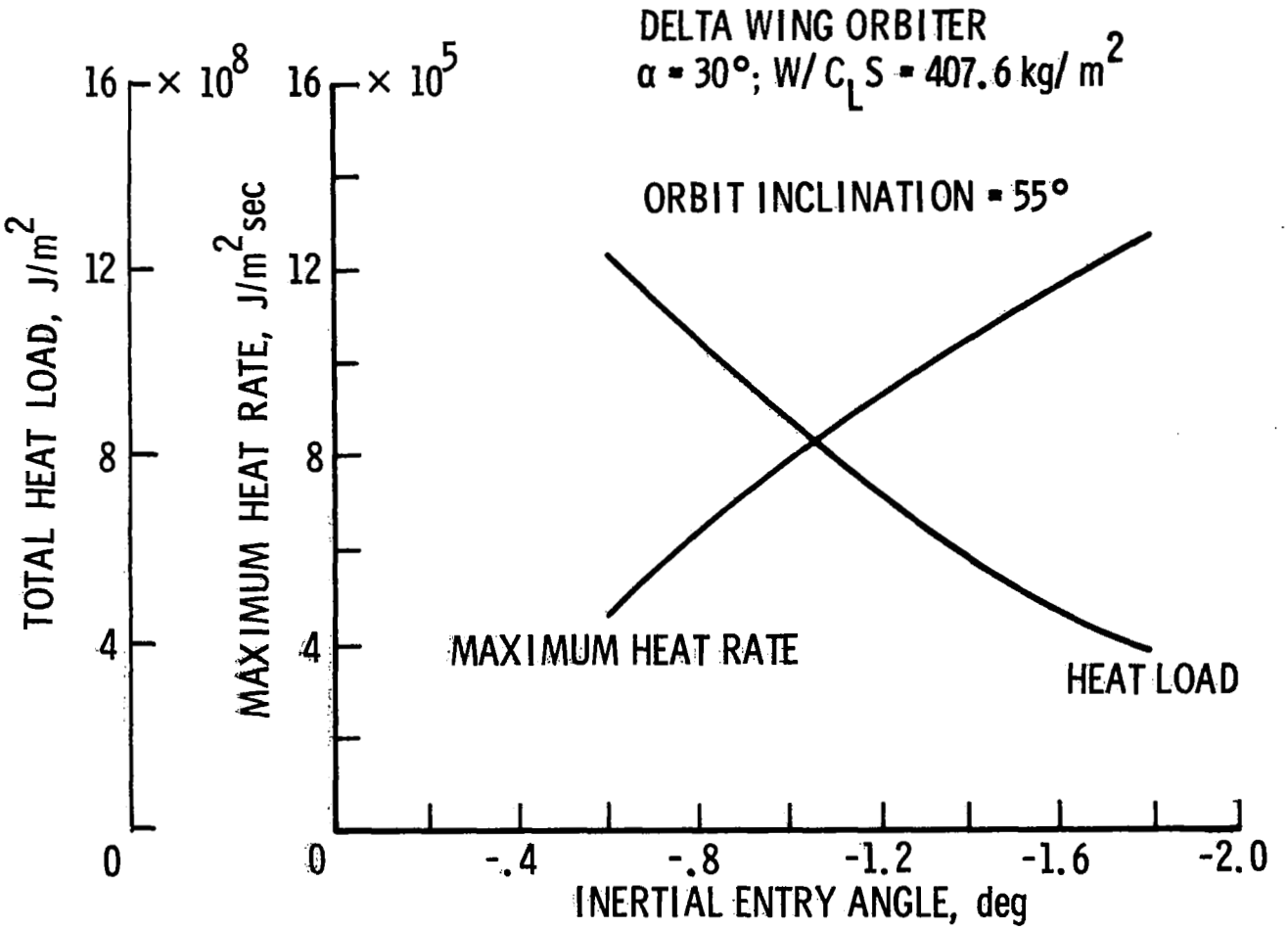

Figure 9

HORIZONTAL IMPULSIVE DEORBIT ΔV REQUIREMENT

To get the desired steeper entry mentioned previously, a greater deorbit ΔV capability is required. Shown in figure 10 is the horizontal impulsive deorbit ΔV requirement for the orbit of interest. The trade between reduced TPS weight and greater deorbit ΔV capability must be investigated.

HORIZONTAL IMPULSIVE DEORBIT ΔV REQUIREMENT

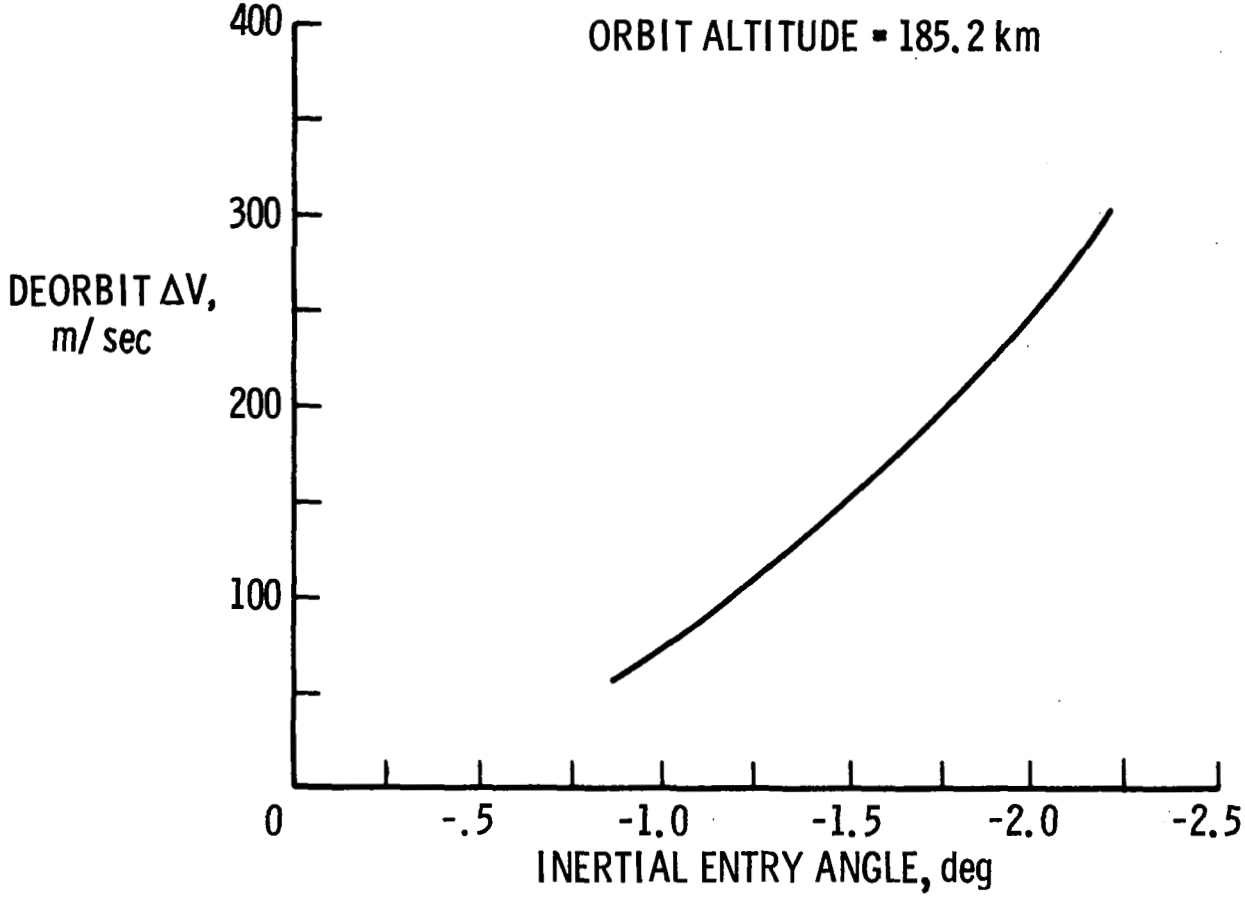

Figure 10

EFFECT OF DEORBIT ΔV ON TOTAL STAGNATION-POINT HEAT LOAD

Minimum total stagnation-point heat-load trajectories were determined for a range of values of deorbit ΔV and cross range. A constant angle of attack was assumed for each cross range, while bank angle was used to optimize the trajectories. As shown by the solid curves in figure 11, the total heat load decreases with increasing deorbit ΔV, for an initial bank angle of 0°.

An alternate approach to achieving the benefits of steeper entry without paying the penalty of increasing deorbit ΔV is the use of negative lift through bank-angle control. That is, by banking the vehicle 180° at entry, the aerodynamic lift forces are utilized to steepen the flight path. The symbols on the figure illustrate the reductions in total heat load resulting from negative lift which can be achieved for one value of ΔV with cross ranges of 300 and 700 n.mi. The total heat loads are reduced by about 20 percent over that for 0° bank angle entries. In effect, the negative lift is equivalent to about 75 m/sec of deorbit ΔV.

EFFECT OF DEORBIT ΔV ON TOTAL STAGNATION-POINT HEAT LOAD

MINIMUM TOTAL HEAT TRAJECTORIES; INITIAL BANK ANGLE = 0^0

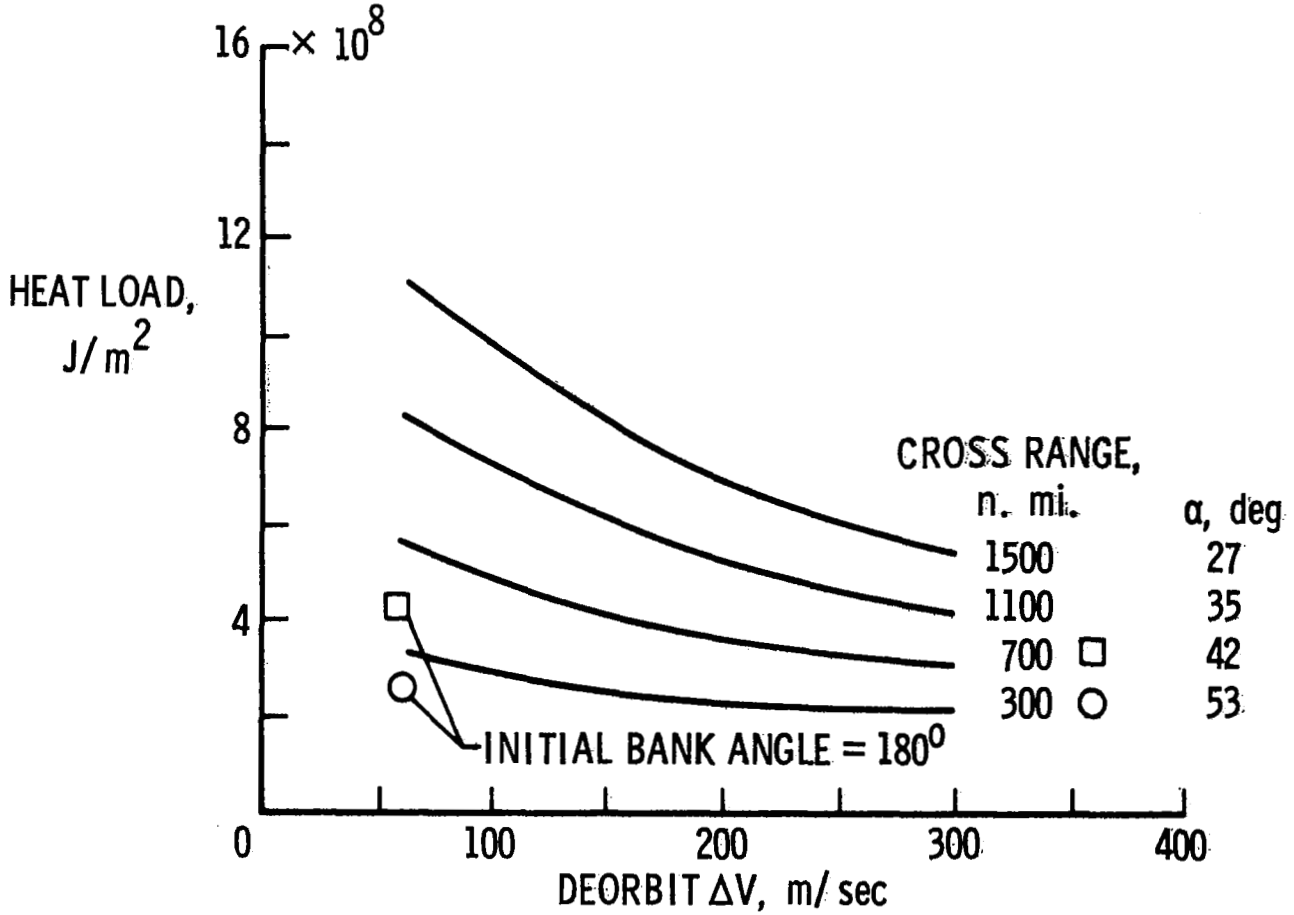

Figure 11

BOTTOM-SURFACE ABLATOR WEIGHT

A preliminary study of the bottom-surface ablator weight for the Mark I orbiter was performed by W. D. Brewer at the Langley Research Center. A heating distribution over the lower surface of a typical delta-wing orbiter was used assuming laminar flow throughout the optimal trajectories determined previously. For the lower values of heat load, a potential for significant ablator-weight savings is seen. (See fig. 12.)

BOTTOM-SURFACE ABLATOR WEIGHT
LAMINAR FLOW ASSUMED

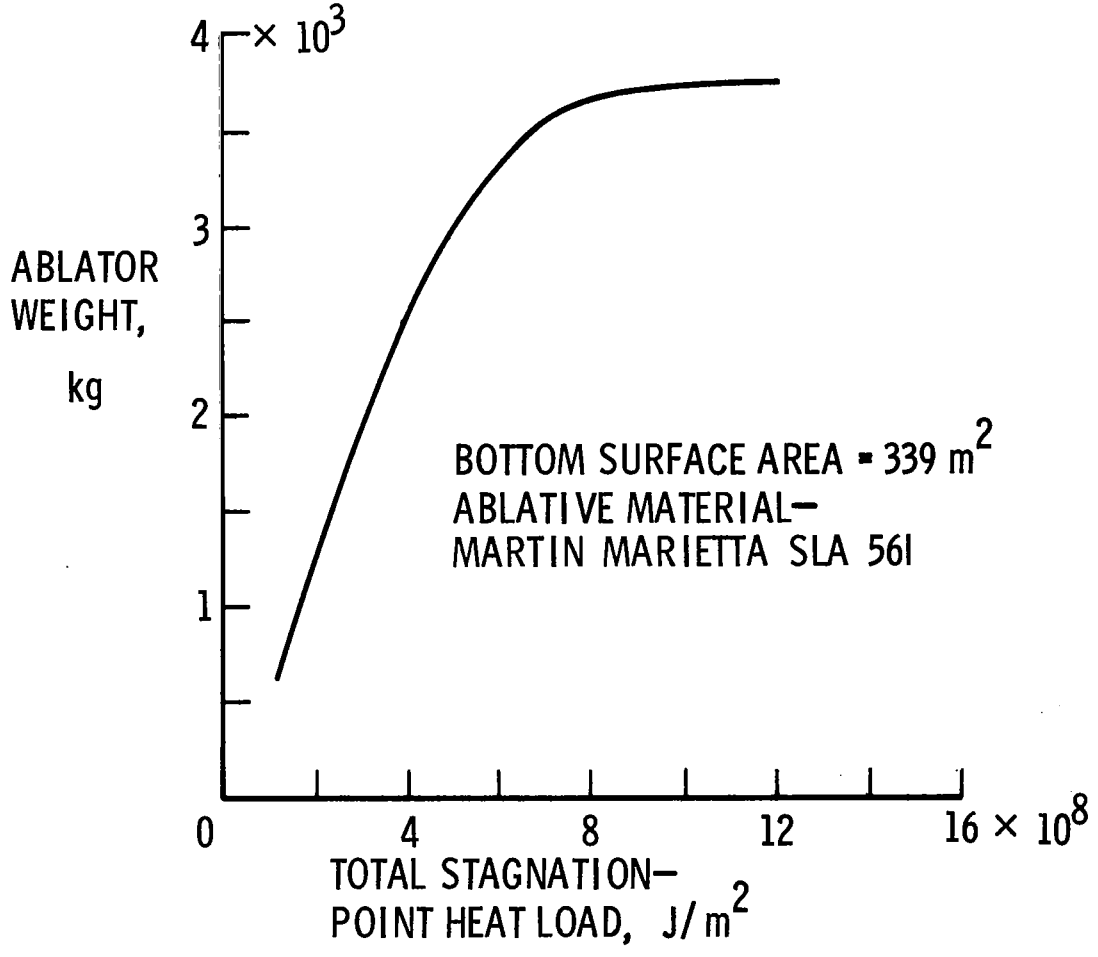

Figure 12

EFFECT OF DEORBIT ΔV ON BOTTOM-SURFACE ABLATOR WEIGHT

By using the total stagnation-point heat load from the optimal trajectories and the results of the preliminary weight study presented in figures 11 and 12, respectively, the effect of deorbit ΔV on the ablator weight is shown in figure 13. For all the values of cross range considered, the bottom-surface ablator weight decreases with increasing ΔV. The greater weight savings occur for the lower values of cross range and ΔV.

EFFECT OF DEORBIT ΔV ON BOTTOM-SURFACE ABLATOR WEIGHT
MINIMUM TOTAL HEAT TRAJECTORIES

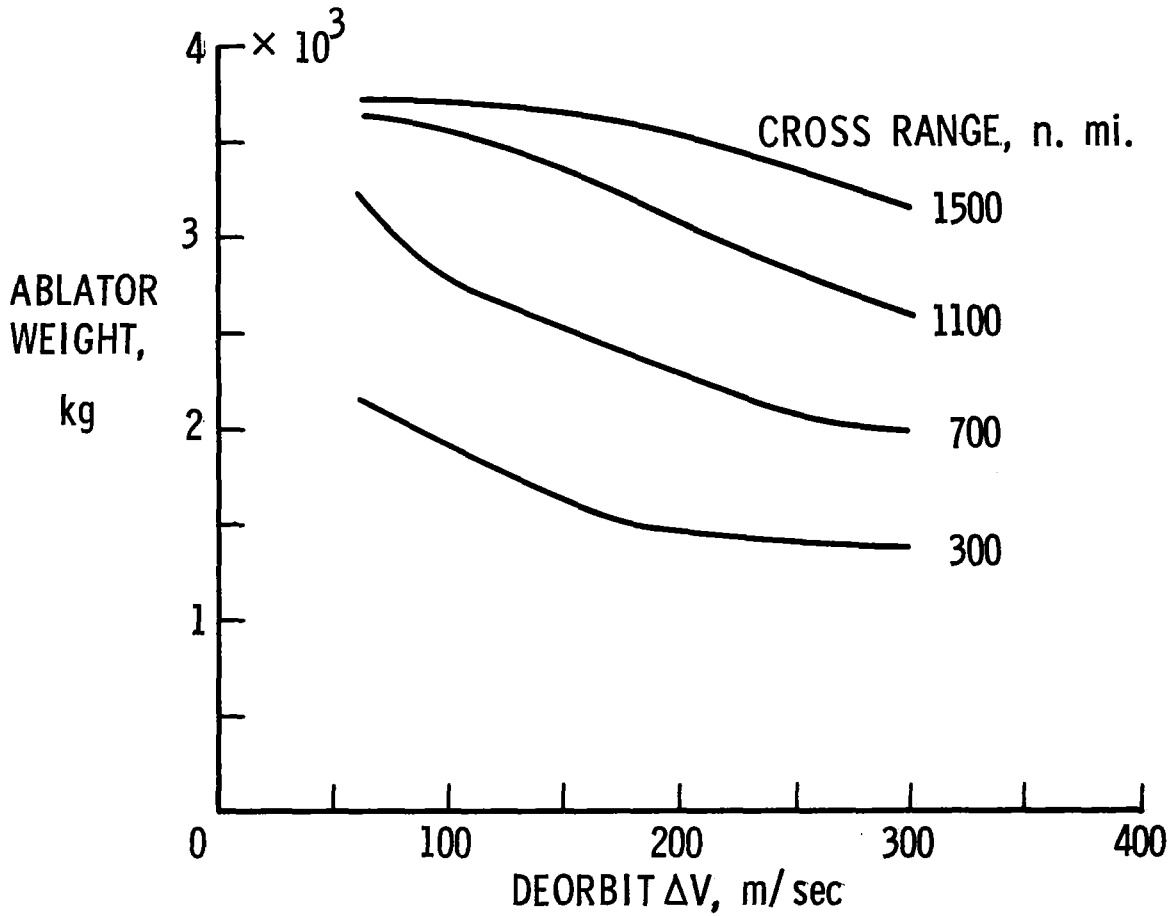

Figure 13

DEORBIT PROPELLANT WEIGHT SUMMARY

While it has been shown that ablator weight is reduced by increasing deorbit ΔV, a propellant weight penalty must be payed for the additional ΔV capability required. Shown in figure 14 is the weight of propellant required to obtain various values of ΔV for a typical orbiter deboost engine. Propellant weight increases with deorbit ΔV at a rate of approximately 17 $\frac{kg}{m/sec}$.

DEORBIT PROPELLANT WEIGHT SUMMARY

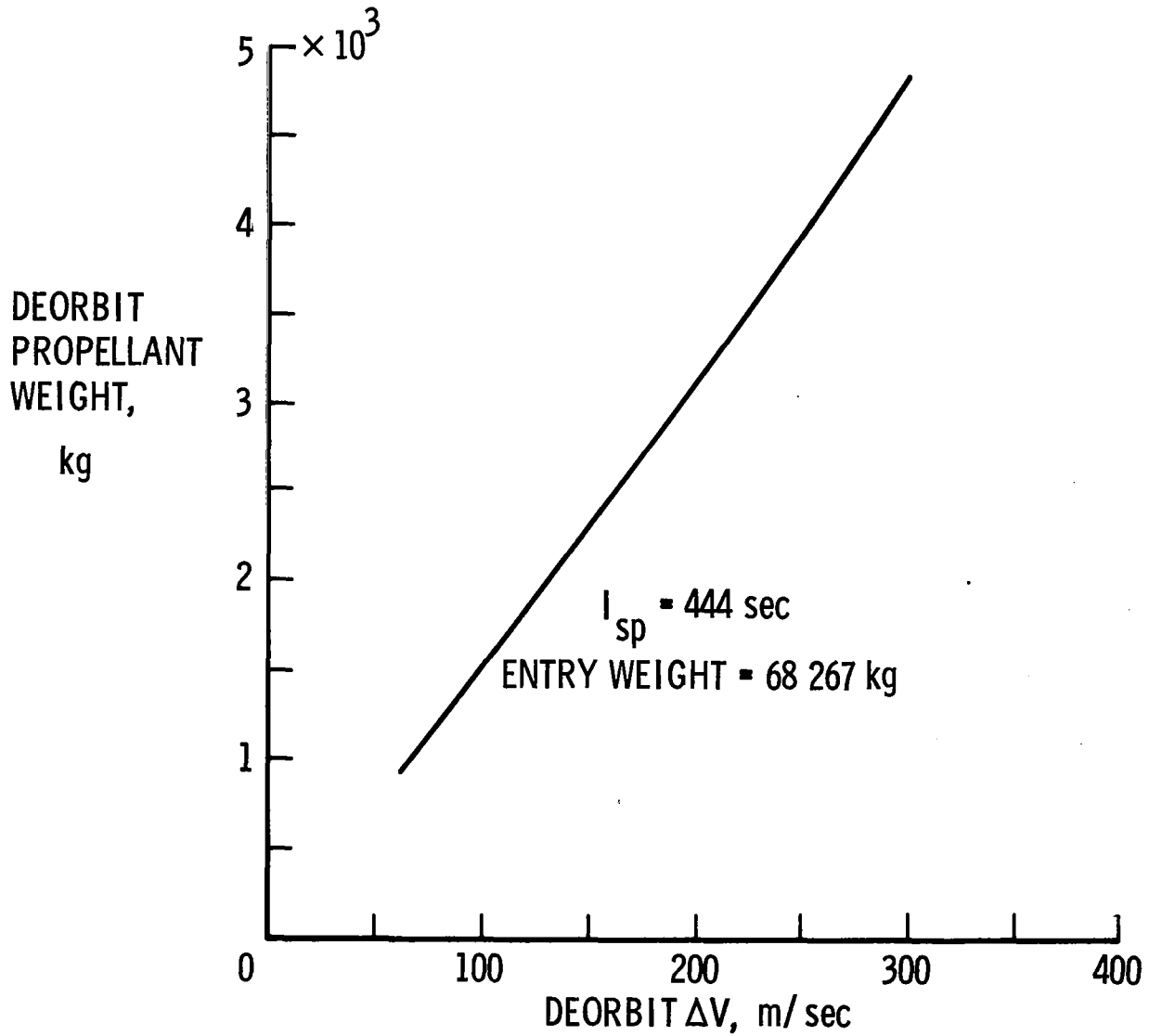

Figure 14

EFFECT OF DEORIBT ΔV ON THE TOTAL OF ABLATOR WEIGHT + DEORBIT PROPELLANT WEIGHT

To find a minimum of the total of the ablator and deorbit propellant weights, the results of figures 13 and 14 are added. As shown by the curves in figure 15, this total weight strictly increases with increasing deorbit ΔV for all values of cross range. Therefore, the vehicle requires only a minimum of deorbit ΔV propellant to achieve the lowest weight even though the advantage of a steeper entry for reducing ablator weight is lost.

To capitalize on the advantage of steeper entry while retaining the low ΔV requirement, the results of entering with the vehicle banked at 180° to achieve a steeper entry by negative lift are also shown in figure 15. The result, denoted by the symbols in the figure, was a 15 percent reduction in the total weight using this entry mode for cross ranges of 300 and 700 n.mi. without violating the 2.5g maximum deceleration limit.

EFFECT OF DEORBIT ΔV ON THE TOTAL OF ABLATOR WEIGHT + DEORBIT PROPELLANT WEIGHT

INITIAL BANK ANGLE = 0^0

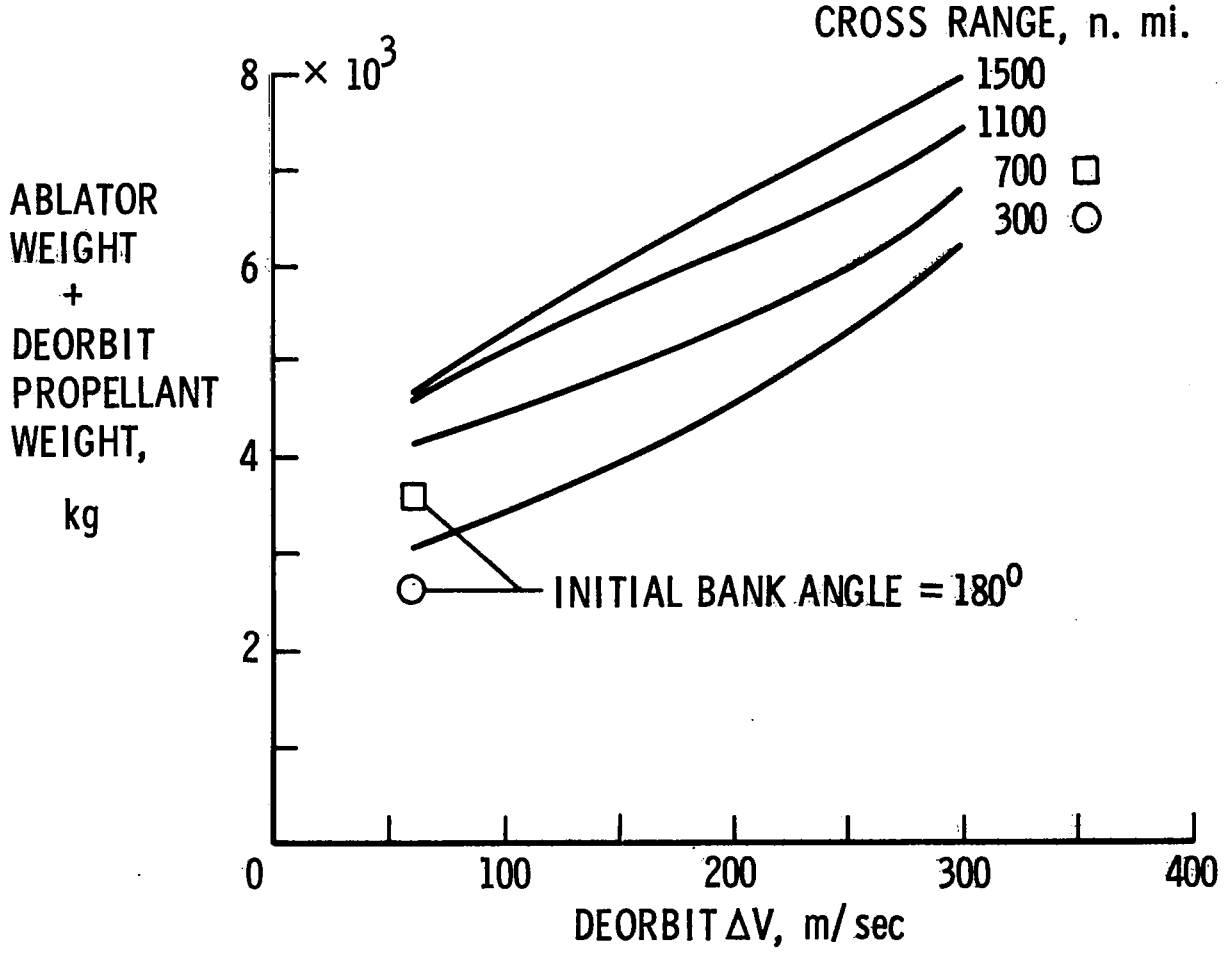

Figure 15

CONCLUDING REMARKS

From a chosen nominal trajectory, significant improvement in shuttle orbiter cross range can be made with no increase in the values of heat load and maximum heat rate at the stagnation point. However, along the bottom center line of the vehicle, a uniform increase of about 10 percent in the values of maximum temperature and total heat load results when using the MDAC boundary-layer transition criteria. Also, the magnitudes of these parameters predicted by the MDAC and NAR criteria were significantly different.

Although the first study considered only a reusable TPS for the orbiter, the results are equally applicable to an ablative TPS. Additional cross-range capability could be obtained with a minimal increase in ablator weight.

While total stagnation-point heat load for the Mark I orbiter can be reduced by increasing deorbit ΔV, the resulting decrease in ablator weight is overcome by the increase in deorbit propellant weight. However, a small deorbit ΔV combined with negative lift in the initial phase of entry results in significant ablator-weight reductions. Negative-lift entry offers a means of saving ablative TPS weight through steepening the entry without a deorbit propellant penalty. The effective reduction of deorbit ΔV obtained using the negative-lift entry mode is equivalent to about 1300 kg of deorbit propellant.

A more detailed ablative heat shield weight study is needed which includes the effects of boundary-layer transition and angle of attack on heating, and structure and insulation weights.